Molecular Crystals and Liquid Crystals
Publication details, including instructions for authors and subscription information:
http://www.tandfonline.com/loi/gmcl16

Polymorphism and Spectroscopic Characterization of an Azo-Pigment: (Pigment Red 31, C.I. 12360)

C. H. Griffiths [a] & A. R. Monahan [a]
[a] Xerox Webster Research Center, Webster, New York, 14580
Version of record first published: 28 Mar 2007.

To cite this article: C. H. Griffiths & A. R. Monahan (1976): Polymorphism and Spectroscopic Characterization of an Azo-Pigment: (Pigment Red 31, C.I. 12360), Molecular Crystals and Liquid Crystals, 33:3-4, 175-187

To link to this article: http://dx.doi.org/10.1080/15421407608084293

Mol. Cryst. Liq. Cryst., 1976, Vol. 33, pp. 175–187

Printed in Holland

Polymorphism and Spectroscopic Characterization of an Azo-Pigment

(Pigment Red 31, C.I. 12360)

C. H. GRIFFITHS and A. R. MONAHAN

Xerox Webster Research Center, Webster, New York 14580

(*Received August 22, 1975*)

The preparation and characterization of the amorphous (A) and three crystalline polymorphs (I, II, III) of the 1-phenylazo-2-naphthol magenta colorant (Pigment Red 31) is described. The polymorphs were identified by x-ray diffraction, calorimetry and absorption and emission spectroscopy.

Heats of transformation measured calorimetrically for A → I, I → III and II → III are 1.80 cals/gram, 3.77 cals/gram, and < 0.2 cals/gram respectively.

The electronic absorption and emission spectra reveal distinct differences among the solid state polymorphs. The electronic spectrum of the amorphous form can be interpreted in terms of a monomeric hydrazone tautomeric structure while the crystalline polymorphs indicate an aggregated hydrazone structure with an increase in intermolecular interaction on going from phase I to the phase III structure.

INTRODUCTION

Pigment Red 31 (4-[2-methoxy-5-benzamidophenylazo]-3′-hydroxy-2′-*N*-(*m*-nitrophenylnaphthamide) represents one of the oldest commercially available magenta pigments.[1] The structural formula of the material in the quinone-hydrazone tautomeric form is shown in Figure 1. The general class of pigment compounds are extremely lightfast and their commercial importance lies in applications for the coloration of paints, printing inks, plastics, etc. More recently, attention has been given to the electrical conductivity,[2] photoconductivity,[2] and solid state charge transfer[3] behavior of the 1-phenylazo-2-naphthol class of dyes and pigments.

Considerable work has been reported on the solution and solid state optical properties[4–7] of 1-phenylazo-2-naphthols however only a limited number of studies have been concerned with crystal structure and polymorphism[8,9] of this class of materials. Reported here is an x-ray, thermal

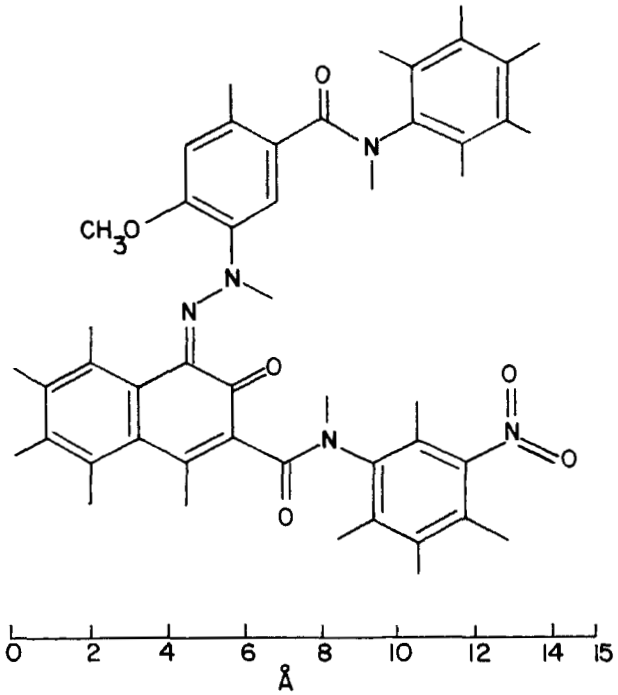

FIGURE 1 Molecular structure of Pigment Red 31.

and optical characterization of four separate Pigment Red 31 phases. Understanding the spectral properties in amorphous and crystalline phases is important to such matters as color control in this important pigment and to its electrical behavior as well.

EXPERIMENTAL

The Pigment Red 31 (C.I. 12360) (Figure 1) used in this study was synthesized[10] by diazotization of 3-amino-*N*-methoxybenzanilide with hydrochloric acid and sodium nitrite. A pyridine solution of the coupler (Naphthal AS—BS) was run into the cold diazonium solution, resulting in a suspension of the pigment. The product was purified by recrystallization from dimethylformamide. Elemental analysis gave C, 65.99%; H, 4.10%; N, 12.56%, compared to the values calculated from the molecular formula of C, 66.35%; H, 4.06%; N, 12.48%. Pigment Red 31 crystals were grown under equilibrium conditions by recrystallization on slow cooling from a number of solvents including dimethylformamide (DMF), isopherone and pyridine.

Attempts to grow crystals from the vapour phase under equilibrium conditions by maintaining a suitable temperature gradient in an evacuated quartz tube were unsuccessful due to decomposition. The material was precipitated in the solid state under non-equilibrium conditions by adding a solution in pyridine and *N*-benzyltrimethyl ammonium hydroxide to water and also by vacuum deposition of a vapour beam onto a cool substrate. The evaporations were carried out at 10^{-5} Torr onto a glass substrate held at ambient temperatures in a Bendix Balzers Model BA-3 evaporator. As there was some doubt as to the role of water in transitions between the different phases, the pigment was also recrystallized from rigorously dried DMF. Water was removed from DMF by addition of triphenyl chlorosilane followed by distillation according to the method described by Thomas and Rochow.[11] The final product contained 0.002% H_2O (Karl Fischer titration) compared with 0.170% in the reagent grade DMF. The results of equilibrium and non-equilibrium deposition were characterized using optical microscopy, x-ray scattering, differential scanning calorimetry and ultraviolet and visible absorption and emission spectra. X-ray diffraction patterns were recorded on Debye Scherrer cameras for all materials and on precession and Weissenberg cameras where growth under equilibrium conditions gave crystals of suitably large size. Calorimetry was carried out using a Dupont 900 Differential Thermal Analyzer with a Differential Scanning Calorimeter (DSC) Cell. Weighed samples in hermetically sealed pans were used and the areas under the transition peaks measured with a compensating planimeter.

Ultraviolet and visible absorption and emission spectra were recorded on a Cary 14 Recording Spectrophotometer and an Aminco-Bowman Spectrophotofluorimeter. Emission spectra were corrected for variations in detector sensitivity with wavelength. Film thickness measurements of evaporated pigment layers were made with a Sloan M-100 Angstrometer.

RESULTS

a Morphology and Crystal Structure

Only the equilibrium methods of preparation produced crystals with a well defined morphology (equilibrium crystalline phase). Solvent growth produced red prismatic needles with lengths up to 3 mm and rectangular cross section with dimensions up to 0.2 × 0.05 mm. Samples of these crystals were studied in detail using precession and Weissenberg cameras. They were found to be monoclinic with the $P2_1$ space group and have lattice dimensions $a = 28.102$ Å, $b = 5.069$ Å, $c = 9.109$ Å and $\beta = 93.48$ Å. This corresponds to a unit cell containing two molecules and a crystallographic density of 1.44 grams/cc.

Non-equilibrium growth by quenching the pyridine solution in water produced a crystalline phase with an irregular platelet structure and a crystallite size of less than 0.02 mm diameter (non-equilibrium crystalline phase). The size was too small for single crystal structure analysis. When the phase was heated in water to 90°C, however, it underwent a phase transition and gave an x-ray diffraction pattern identical to that from the equilibrium crystalline phase grown from solution under equilibrium conditions.

Quenching from the vapour phase produced a compact structureless film which was determined by polarizing microscopy and x-ray scattering to be completely amorphous (non-equilibrium amorphous phase). These amorphous Pigment Red 31 films were extremely stable (> 1 year) under ambient environmental conditions.

b Calorimetric Measurements

The three forms of Pigment Red 31 discussed above were studied by differential scanning calorimetry over the temperature range of 25–350°C. The bulk amorphous phase was obtained by scraping off the amorphous films from the glass substrate. Thermal reactions were identified by x-ray scattering from the thermally quenched products. Figure 2 shows typical thermograms produced at a heating rate of 20°C/minute. It was found that on heating, the bulk amorphous phase transformed rapidly at approximately 90°C into the

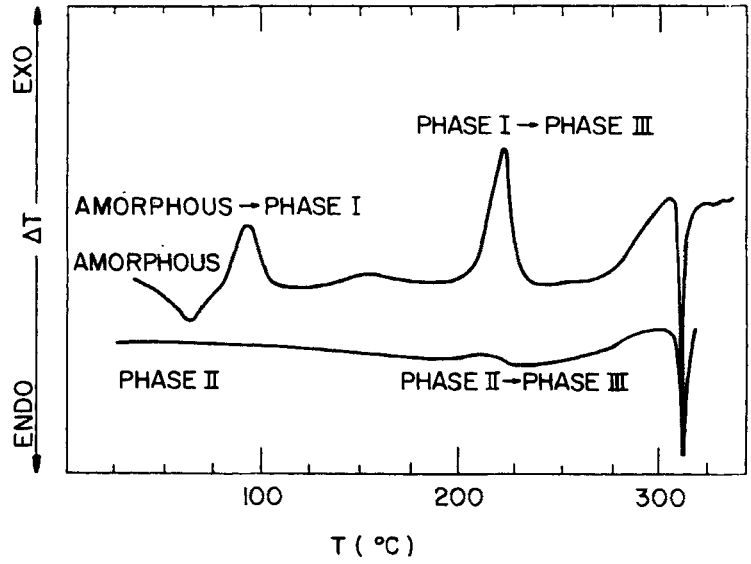

FIGURE 2 DSC traces showing phase transitions.

non-equilibrium crystalline phase discussed above. On further heating this latter phase transformed rapidly at approximately 225°C into a previously unidentified phase. No further transitions, only increases in crystal size and perfection, were observed up to the melting point of approximately 320°C. The phase transitions observed are identified by the exothermic peaks in thermogram (*a*) of Figure 2. As expected the non-equilibrium crystalline phase prepared by precipitation from solution gave the single exothermic peak at approximately 225°C, to produce again the unidentified phase discussed above and finally melted at $\approx$320°C. It behaved in an identical manner to the same phase formed by heating the amorphous pigment to 90°C. Some inconsistencies in peak heights and positions were encountered with the amorphous pigment. This was traced to decomposition occurring when the evaporation boat temperature was not controlled closely enough during the vacuum deposition step.

The phase produced by recrystallization from solvents under equilibrium conditions and by heating phase I to 90°C in water did not appear in any part of the amorphous-through-to-melt sequence described above. Thermograms obtained from this material indicated no strongly exothermic or endothermic transitions up to the melting point. X-ray scattering however indicated a phase transition occurring between 200 and 225°C to give again the same unidentified phase produced from the non-equilibrium crystalline phase at this temperature. The thermogram shows only a very weak exothermic hump in this temperature region.

The energies involved in the phase transitions discussed above were calculated from the integrated areas under the transition peaks of the thermograms using the formula

$$\Delta H = \frac{E \cdot A \cdot \Delta T_s \cdot T_s}{M \cdot a}$$

where E is the calibration coefficient, A the transition peak area, ΔT_s and T_s the y and x axis sensitivities respectively, M the sample mass and a the heating rate. The calibration coefficient was determined from thermograms of samples with known heats of fusion recorded under identical conditions to the Pigment Red 31 thermograms.

Table I shows the energies of the phase transitions and the temperatures corresponding to the maxima in the exothermic transition peaks. The melting point given is that indicated by the extrapolated onset. For the sake of clarity the non-equilibrium crystalline phase, the equilibrium crystalline phase and the high temperature crystalline phase have been named Phase I, II and III respectively, in order of their appearance when the amorphous phase was heated. The thermal phase reactions and corresponding x-ray scattering patterns are similarly identified in Figures 2 and 3. Like the

TABLE I

Phase reactions of pigment red 31

Transformation	ΔH cal/gm	$T°C^a$
Amorphous $\longrightarrow$ Phase I	1.80 ± 0.10	90
Phase I $\xrightarrow{H_2O}$ Phase II	?	<90
Phase I $\longrightarrow$ Phase III	3.77 ± 0.07	220
Phase II $\longrightarrow$ Phase III	<0.2	220
Phase III $\longrightarrow$ melt	—	334[a]

[a] Material crystallized from isopherone.

calorimetric data, the x-ray scattering patterns indicate a major reorganization in passing from Phase I to Phase III, but relatively minor differences between Phases II and III.

As previously stated the direct transition from Phase I to Phase II could not be produced thermally although it was known to occur in the presence of water. Sealing Phase I with distilled water in a hermetic seal DSC sample container and subjecting the sample to a programmed heating cycle in the calorimeter cell confirmed that the Phase I → Phase II transition did occur at a temperature below 100°C in the presence of water. In order to determine whether water was incorporated into the Phase II lattice both Phase I and Phase II Pigment Red 31 were recrystallized from rigorously dried (0.002% H_2O) DMF and reagent grade DMF. In each case the recrystallized material was Phase II and Phase II material was shown to crystallize from DMF in the absence of H_2O.

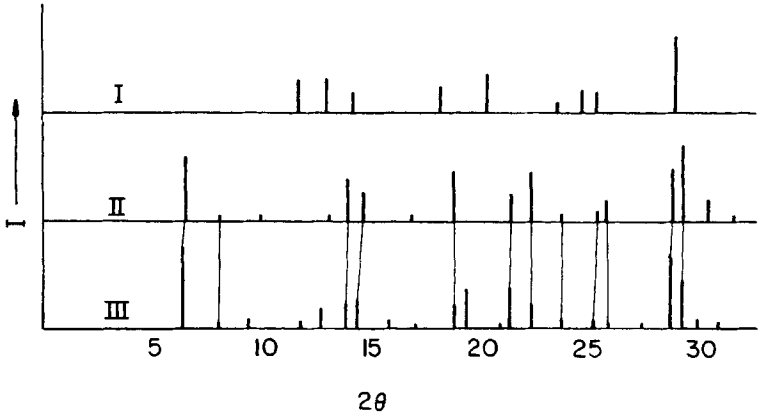

FIGURE 3 X-ray scattering from the crystalline phases of Pigment Red 31.

c Visible Absorption and Emission Spectra

Visible absorption spectra were measured at room temperature using the Nujol mull technique. The spectra were recorded on the same quenched samples used to obtain the x-ray powder patterns. The resultant spectra normalized to optical density of 1.0 are shown in Figure 4. The corresponding

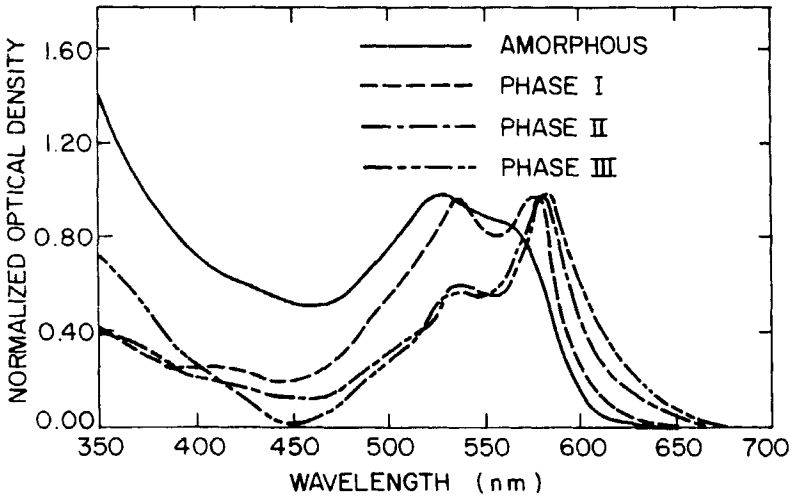

FIGURE 4 Absorption spectra from Pigment Red 31 using the "Nujol" mull technique.

molecular absorption band measured in dimethylformamide (DMF) is shown for comparison in Figure 5.

The absorption maximum of the unheated amorphous material occurs at ca. 530 nm and the absorption coefficient of this electronic transition is 6.0×10^4 cm^{-1}.† At 90°C the absorption maximum shifts to 575 nm ($\alpha = 6.8 \times 10^4$ cm^{-1}). Continued heating to 220°C results in a further shift of the long wavelength maxima to 580 nm. Associated with the spectral shift is an increase in absorption coefficient of the transition to 7.2×10^4 cm^{-1}.

Room temperature fluorescence spectra were also measured for the four polymorphs. Nujol mulls of the material were coated on a quartz window and excited with 500 nm radiation. The fluorescence emission was viewed normal to the front surface of the quartz windows. Fluorescence spectra are shown in Figure 6. The emission from the amorphous and three crystalline

† Using a crystal density of 1.44 and the solution molar extinction coefficient of 2.1×10^4 l $mole^{-1}$ cm^{-1}, an absorption coefficient of 5.4×10^4 cm^{-1} is calculated which is in reasonable agreement with the measured value.

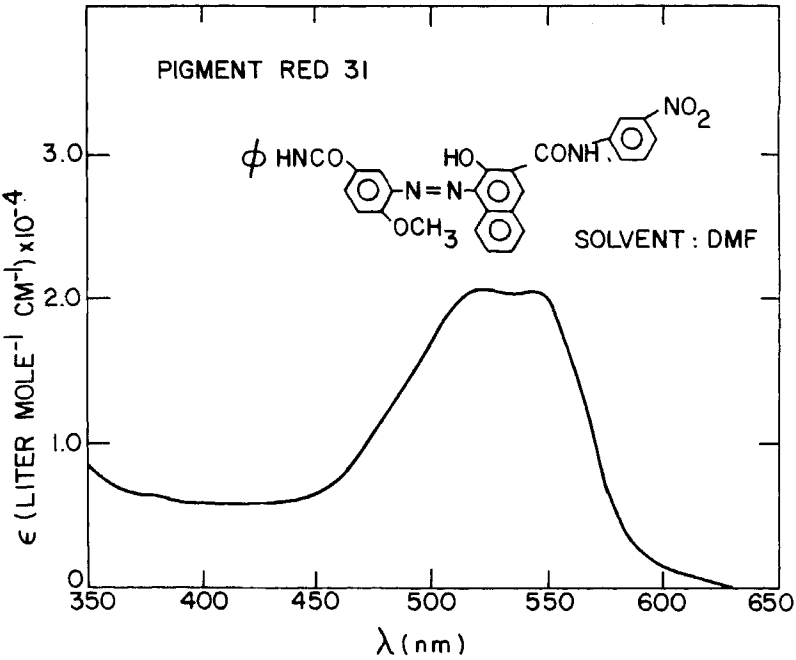

FIGURE 5 Molecular absorption spectrum from Pigment Red 31.

forms of Pigment Red 31 are shifted to longer wavelengths in the order amorphous < I < II < III. Structure was absent in the spectra at room temperature to within the 2 nm resolution of the instrument.

DISCUSSION

The calorimetric data presented above clearly indicate that Pigment Red 31 can exist in the amorphous state and as three distinct crystalline phases. Both the amorphous phase and Phase I, the non-equilibrium crystalline phase, required rapid non-equilibrium condensation from the molecular state for their formation. The extremely efficient technique of vapour beam quenching was required to produce the amorphous phase but once formed this material was found to be quite stable. The less efficient technique of rapid precipitation from solution produced the more ordered Phase I crystalline material. Equilibrium condensation from the molecular state produced Phase II, the stable crystalline phase which then transformed at approximately 220°C to Phase III with very little change in enthalpy.

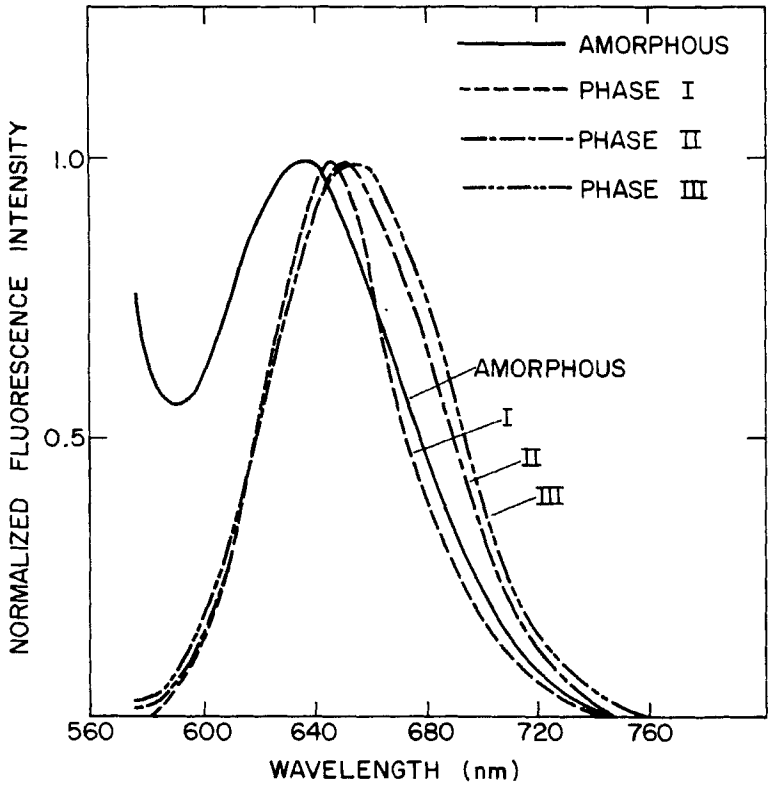

FIGURE 6 Fluorescence spectra from Pigment Red 31 in a "Nujol" mull.

The energies of the exothermic transitions from the two non-equilibrium phases to Phase III give a clear indication of the relative stabilities of these structures (Table I). The relationship of Phases II and III and the reasons for the transitions from Phase I → Phase II in the presence of water rather than Phase I → Phase III in the absence of water are less obvious. As stated previously the x-ray diffraction patterns from Phases I, II and III indicate a major reorganization in structure in passing from Phase I to Phase II and III but only minor differences between II and III. These differences are restricted to changes in line intensities and small changes in line position plus the appearance of a few new diffraction lines. It would seem that the Phase III structure is only slightly different from the monoclinic Phase II structure and is a high temperature variant of the Phase II structure. However attempts to interpret the Phase III pattern in terms of the basic Phase II pattern and structural defects, twinning, etc. were unsuccessful. As Phase II is formed from solution under equilibrium conditions and by the transformation of Phase I

at approximately 100°C (heating with water) it seems a reasonable assumption that Phase II is the stable phase at room temperature and up to 100°C. In the absence of water, Phase I transforms at a higher temperature (~200°C) and goes to Phase III. Phase II also transforms to Phase III at this same temperature. It would seem that at ~200°C Phase III is the stable phase. The actual structure of Phase III is not known and its determination awaits the development of techniques for the growth of suitable single crystals for x-ray structure determination.

The visible electronic spectra of solution and amorphous phases of Pigment Red 31 relative to the crystalline forms give definite indications that strong intermolecular interactions are operative in the crystalline solid state.[7] The observation that amorphous and crystalline phases of organics show different spectral properties is not new. Indeed, the 600–700 Å spectral red shifts for crystalline indigo[12] relative to the dissolved dye or the amorphous solid are an example of differences in hydrogen bonding interactions in crystalline and amorphous phases of organics. Maruyama and Iwasaki[13] have recently reported an electronic spectrum of naphthacene in both amorphous film form and in the crystalline solid. The amorphous film spectrum is similar to electronic spectra in neutral solutions whereas the crystalline solid reveals Davydov splittings in the electronic absorption spectrum resulting from strong intermolecular interactions. The spectral properties of Pigment 31 are similar to Indigo in that the solution and amorphous solid spectra are both indicative of absorption due to isolated molecules whereas the crystalline solid is observed to undergo a spectral red shift suggestive of aggregation phenomena.

A novel feature of the class of 1-phenylazo-2-naphthols (of which Pigment Red 31 is a member) is the existence of a quinone-hydrazone $\rightleftharpoons$ azo-enol equilibrium. The tautomeric equilibrium for 1-phenylazo-2-naphthol is:

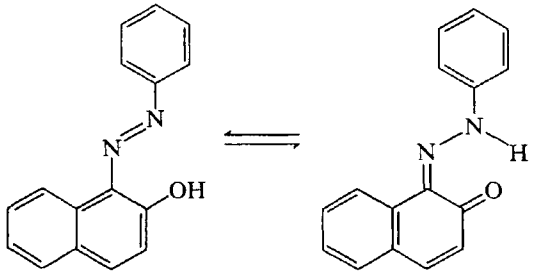

azo — λ max $\simeq$ 420 nm

hydrazone — λ max $\simeq$ 500 nm

The position of the equilibrium is sensitive to solvent and substituents on the aromatic rings.[14,15] Previous work[4,5] has shown that the hydrazone

structure predominates in 1-phenylazo-2-naphthol and electron withdrawing groups, i.e., amide, carboxylate, etc. ortho to the OH moiety stabilize the hydrazone structure and in fact direct the equilibrium entirely in favor of the hydrazone. In the absence of hydrazone directing substituents, i.e., 1-phenylazo-2-naphthol, both tautomers are observed spectroscopically in solution (Figure 7), however, adsorption onto silica-gel substrates results in complete conversion to the hydrazone tautomer.[16] Thus, the electronic

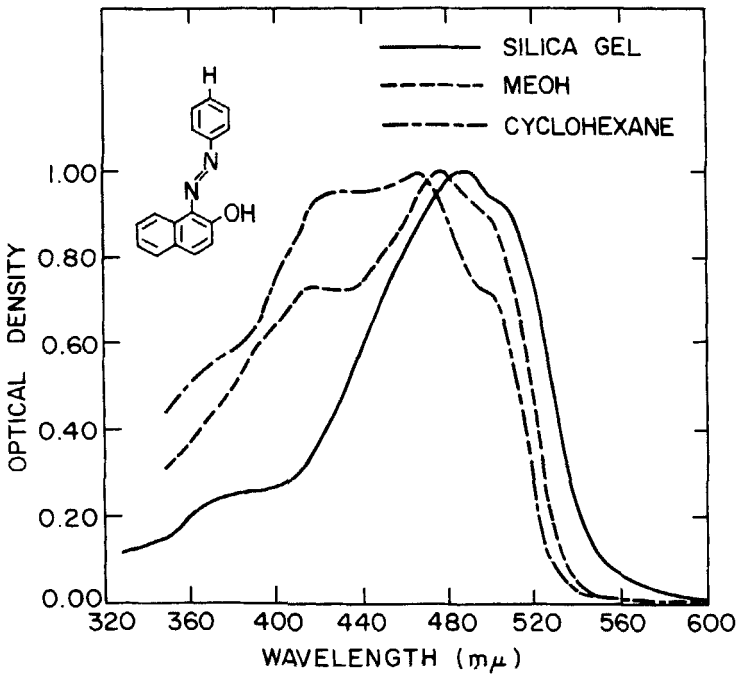

FIGURE 7 Absorption spectra of 1-phenylazo-2-naphthol showing quinone and hydrazone tautomers.

transitions of the hydrazone tautomer are characterized by an intense band at *ca.* 500 nm and a weak second electronic transition[15] at *ca.* 400 mμ. These two hydrazone transitions are observed (Figure 5) at 530 mμ and 425 mμ respectively for Pigment Red 31 in DMF and in Figure 4 for the amorphous phase.

On the basis of past work, the spectral red shift in Pigment Red 31 upon crystallization is believed to have its origin in molecular aggregation phenomena. The spectral shift may be understood qualitatively by the molecular exciton model advanced by McRae and Kasha.[17] The shifts in the crystalline states suggest that the Pigment Red 31 hydrazone molecules are packed

in a card-pack fashion. The fact that the crystalline transitions are red shifted relative to the monomer (amorphous or solution) indicates that the array of molecules are slightly tilted† in the deck.[17] The tilt angle between molecules is measured between the line connecting the centers of molecules and the axes of the transition dipoles. The parallel or card-pack structure seems quite feasible for large planar pigment molecules such as Pigment Red 31. Thus the spectra of Phase I, II and III are interpreted on the basis of a resonance interaction of excited states of coupled aggregates. The increasing red shift indicates an increase in intermolecular interaction on going from Phase I to II to III.

This picture is not at variance with the crystallographic data developed for the Phase II structure. The phenylazonaphthols like other large basically planar organic molecules usually form stacks of parallel molecules in their crystals with the stacking axis parallel to a particular crystallographic axis.[8,9] The $P2_1$ space group indicates that the two molecules in the unit cell are related by a rotation of 180° about the *b*-axis and a displacement of $b/2$ parallel to it. These two symmetry related molecules will be members of two different stacks where the molecular spacing is 5.069 Å along the *b*-axis. The molecules in one stack will be 5.069 Å/2 out of phase with the 2nd stack and the molecules in one stack will be either parallel with those in the second stack (and normal to the *b*-axis) or equally and oppositely inclined to the *b*-axis. A possible stacking configuration is shown in Figure 8. The *c*-axis dimension is smaller than any of the molecular plane dimensions shown in Figure 1 and indicates that the molecules must be tilted with respect to both *c* and *b*-axes (the angle between the *c* and *b*-axes = 90°).

The finer details of the packing of the Pigment Red 31 molecules in the Phase II structure are unknown at this time and the structures of Phase I and III are even less understood. Nevertheless the calorimetric data indicate in agreement with the optical data that the packing of molecules is looser in Phase I than Phase II and slightly tighter in Phase III.

The shift in crystal fluorescence maxima to longer wavelengths in the order III < II < I < amorphous also indicates an increase in intermolecular interaction.[18] The increase in intermolecular interaction could possibly result from a closer molecular spacing or greater overlap of adjacent molecules on going from the amorphous to the Phase I to II to III structure. Previous studies[19] relative to the luminescence properties of 1-phenylazo-2-naphthols demonstrated azo molecular structures to be non-fluorescent and that emission can be ascribed solely to hydrazone tautomeric structures. This finding adds further support to our conclusion that hydrazone structures dominate the polymorphic variations of Pigment Red 31.

† A blue shift would be indicative of a highly tilted deck.[16]

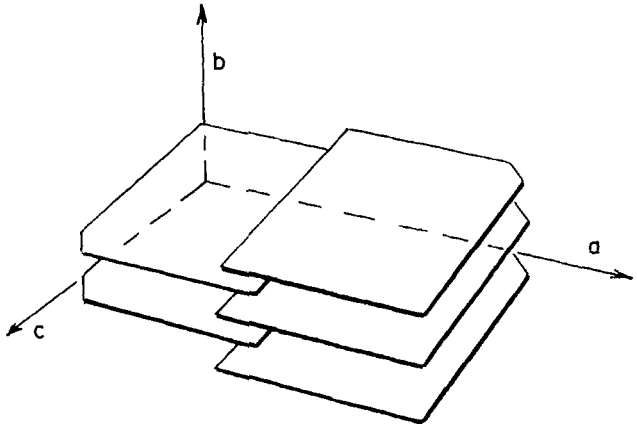

FIGURE 8 Possible molecular stacking configuration in Pase II Pigment Red 31.

Acknowledgements

The authors would like to acknowledge the help of N. Germano who supplied the pigment samples, P. Goldstein who determined the unit cell parameters of the Phase II structure and A. DeLuca and P. Vernon for assistance with the experimental work.

References

1. K. Venkataraman, *The Chemistry of Synthetic Dyes*, Academic Press, Inc., New York, N.Y., 1965, p. 701.
2. H. Rau, *Ber. Bunsenges.*, **73**, 810 (1969).
3. P. J. Cressman, G. C. Hartmann, J. E. Kuder, F. D. Saeva and D. Wychick, *J. Chem. Phys.*, **61**, 2740 (1974).
4. A. R. Monahan and D. F. Blossey, *J. Phys. Chem.*, **74**, 4014 (1970)).
5. A. R. Monahan, N. J. Germano and D. F. Blossey, *ibid.*, **75**, 1227 (1971).
6. A. R. Monahan, A. F. DeLuca and A. T. Ward, *J. Org. Chem.*, **36**, 3838 (1971).
7. A. R. Monahan and J. B. Flannery, Jr., *Chem. Phys. Lett.*, **17**, 510 (1972).
8. C. T. Grainger and J. F. McConnel, *Acta Cryst.*, **B25**, 1962 (1965).
9. Von D. Kobelt, E. F. Paulus and W. Kunstmann, *Acta Cryst.*, **B28**, 1319 (1972).
10. N. Germano, private communication.
11. A. B. Thomas and E. G. Rochow, *J. Amer. Chem. Soc.*, **79**, 1843 (1957).
12. A. R. Monahan and J. E. Kuder, *J. Org. Chem.*, **37**, 4182 (1972).
13. Y. Maruyama and N. Iwasaki, *Chem. Phys. Lett.*, **24**, 26 (1974).
14. G. Gabor, Y. F. Frei, D. Gegiou, M. Kaganowitch and E. Fischer, *Israel J. Chem.*, **5**, 193 (1967).
15. H. Zollinger, *Azo and Diazo Chemistry* (Interscience, New York, N.Y., 1961), p. 311.
16. A. R. Monahan and A. F. DeLuca, to be published.
17. E. D. McRae and M. Kasha, in *Physical processes in radiation biology*, eds. L. Augenstein, R. Mason and B. Rosenberg (Academic Press, New York, N.Y., 1964), p. 23.
18. M. S. Walker, R. L. Miller, C. H. Griffiths and P. Goldstein, *Mol. Cryst. and Liquid Cryst.*, **16**, 203 (1972).
19. D. Gegiou and E. Fischer, *Chem. Phys. Lett.*, **17**, 510 (1972).